Materials Science & Engineering A xxx (xxxx) 141907

Contents lists available at ScienceDirect

Materials Science & Engineering A

journal homepage: www.elsevier.com/locate/msea

Achieving super-high strength and acceptable plasticity for a near β-type Ti-4.5Mo-5.1Al-1.8Zr-1.1Sn-2.5Cr-2.9Zn alloy through manipulating hierarchical microstructure

Xinjie Zhu [a, b, c], Qunbo Fan [a, bc, *], Haichao Gong [a, b], Jiayao Ying [a, b], Hong Yu [a, b], Xingwang Cheng [a, b], Lin Yang [a], Liu Yang [c], Nan Li [d], Jishan Li [d]

[a] National Key Laboratory of Science and Technology on Materials Under Shock and Impact, School of Materials Science and Engineering, Beijing Institute of Technology, Beijing, 100081, China
[b] Beijing Institute of Technology Chongqing Innovation Center, Chongqing, 401135, China
[c] Chengdu Advanced Metal Materials Industrial Technology Research Institute Co. Ltd, Chengdu, 610000, China
[d] China North Vehicle Research Institute, Beijing, 100072, China

ARTICLE INFO

Keywords:
Titanium alloy
Hierarchical microstructure
Super-high strength
Acceptable ductility

ABSTRACT

In the present study, a hierarchical microstructure, which was significantly different from the traditional microstructure of titanium alloys, was prepared by specially designing the solution and aging treatment parameters of a near β-type hot-rolled Ti-4.5Mo-5.1Al-1.8Zr-1.1Sn-2.5Cr-2.9Zn alloy: (1) Firstly, in the process of solution-treatment (920 ˚C/1 h/WQ), a hierarchical microstructure in equiaxed primary α grains (α_p) composed of nano-scale equiaxed α grains (α_{ps}) and β phase embedded between α_{ps} was formed by controlling the diffusion rate of β stable elements in α_p regions. (2) Then, in the process of aging-treatment (550 ˚C/6 h/AC), a hierarchical microstructure composed of acicular secondary α phase (α_s) with a thickness of dozens of nanometers, smaller acicular α phase (α_{ss}) with a thickness of 10 nm, distributed in the space of two α_s, and whisker β phase ($\beta_{whisker}$), was observed in transformed β (β_t) regions. Comparing to the solution-treatment of 900 ˚C/1 h/WQ followed by the same aging-treatment, smaller α_p, a large number of nano-scale equiaxed α_{ps}, and denser and finer acicular α phases were found in the titanium alloy. Due to the combined strengthening effect of equiaxed α_p refinement, nano-scale equiaxed α_{ps} and acicular α phases, the hierarchical microstructure exhibited super-high yield strength of 1255 MPa and ultimate tensile strength of 1420 MPa. Meanwhile, the refined equiaxed α_p and the nano-scale equiaxed α_{ps} could offset the negative effect of acicular α phases on plasticity, hence to maintain the plasticity at an acceptable level (elongation: 6%). Such hierarchical microstructure in the titanium alloy overcame the limitation of the strength-ductility trade-off to a certain extent.

1. Introduction

In recent years, titanium alloys have attracted great attention due to their high strength, good toughness and low density [1,2]. In fact, the excellent mechanical properties, especially the high strength and plasticity of titanium alloys, are mainly determined by complex microstructures [3–5]. Therefore, researches have made great efforts on the microstructure design of titanium alloys [6–10].

Fu et al. [11] designed a microstructure of Ti–15Nb–5Zr–4Sn–1Fe alloy, which was composed of β matrix and nano-scale equiaxed α grains embedded in β matrix, via theoretical composition calculation and hot-rolling followed by annealing heat-treatment. The ultimate tensile strength (UTS) was increased to 972 MPa by grain boundary strengthening mechanism and precipitation strengthening mechanism of ultra-fine grain structure, and the plasticity was maintained at a high level (elongation: 18.4%). Devesh et al. [12] prepared a microstructure

* Corresponding author. National Key Laboratory of Science and Technology on Materials Under Shock and Impact, School of Materials Science and Engineering, Beijing Institute of Technology, Beijing, 100081, China.
E-mail address: fanqunbo@bit.edu.cn (Q. Fan).

https://doi.org/10.1016/j.msea.2021.141907
Received 25 March 2021; Received in revised form 2 June 2021; Accepted 14 August 2021
0921-5093/

composed of micro-scale grains and nano-scale equiaxed grains by the cold-rolling of the ultra-fine grain structure in commercial pure titanium. Due to the fine grain strengthening mechanism of nano-scale grains, the UTS was increased to 990 MPa, and the elongation was maintained at 36%. Daniel et al. [13] fabricated a non-uniform ultra-fine grain structure in commercial pure titanium by hydrostatic extrusion process, and the UTS was increased to 1075 MPa. Other scholars have also exerted themselves to regulating the ultra-fine equiaxed grain microstructures for strengthening titanium alloys [14–16]. However, regulating the ultra-fine equiaxed grain microstructures can only marginally improve the strength of titanium alloys. Significantly, because acicular phase, especially ultra-fine acicular phase, can prominently enhance the strength of titanium alloys [17,18], adjusting the morphology of the ultra-fine acicular phase in titanium alloys has gradually become the research focus of microstructure design. Ivasishin et al. [19] designed a microstructure composed of β grains with an average grain size of 50 μm and acicular secondary α phase (α_s) by the aging-treatment of VT22 alloy at 600 °C for 8 h. The UTS was increased to 1355 MPa, while the elongation was only 2.2%. Wang et al. [20] prepared a microstructure containing nano-scale α_s, primary rod-α phase and β matrix by diffusion-multiple method for Ti–6Al–4V-xMo-yZr ($0.45 < x < 12$, $0.5 < y < 14$, wt. %) alloy. The UTS of the titanium alloy was increased to 1409 MPa by grain boundary strengthening mechanism, while the elongation was only 0.7%. It can be inferred from the above reports that due to the limitation of the strength-ductility trade-off [21,22], although the strength of titanium alloys can be significantly improved by regulating the thickness, aspect ratio and phase fraction of α_s precipitated in transformed β (β_t) regions, the plasticity is dramatically sacrificed at the same time, which indicates the limitation of this method in improving the mechanical properties of materials.

Hierarchical microstructure is an emerging idea applied in designing microstructures to optimize the mechanical properties of titanium alloys [3,23–25]. Kang et al. [26] prepared a bimorphic microstructure composed of typical triangle colonies with ultrafine lamellar α and β, and their border regions with ultrafine equiaxed α, dispersed nano/ultrafine β, as well as α/β interface L layers, in Ti–6Al–4V alloy by powder sintering and in-situ press forging. In their research, due to the resisting effect of ultrafine lamellar microstructure on dislocation motion, the strength of the titanium alloy was effectively improved. Simultaneously, the ultra-fine equiaxed microstructure could store more dislocations, thus maintaining the plasticity at a relatively high level. Therefore, the bimorphic microstructure exhibited excellent mechanical properties, and the yield strength (YS) and elongation were 1138 ± 30 MPa and 19.5 ± 0.5%, respectively. In this paper, inspired by the design idea of bimorphic microstructure, a hierarchical microstructure, which was significantly different from the traditional microstructure of titanium alloys, was obtained by controlling the diffusion rate of β stable elements in equiaxed primary α (α_p) regions during solution-treatment (920 °C/1 h/WQ) and the precipitation process of acicular α phases in β_t regions during the subsequent aging-treatment (550 °C/6 h/AC). The hierarchical microstructure was composed of α_p regions and β_t regions. In α_p regions, the microstructure contained nano-scale equiaxed α grains (α_{ps}) and β phase embedded between α_{ps}. While in β_t regions, the microstructure contained acicular α_s with a thickness of dozens of nanometers, smaller acicular α phase (α_{ss}) with a thickness of 10 nm, distributed in the space of two α_s, and whisker β phase ($\beta_{whisker}$). Moreover, the hierarchical microstructure exhibited super-high strength (YS: 1255 MPa, UTS: 1420 MPa) and acceptable plasticity (elongation: 6%).

2. Experiment procedure

The as-received material utilized in the present study is a near β-type Ti-4.5Mo-5.1Al-1.8Zr-1.1Sn-2.5Cr-2.9Zn alloy ingot prepared via triple melting in a vacuum arc remelting furnace. The chemical composition is analyzed by wet chemical method, and the corresponding result is listed in Table 1. The β-transus temperature (T_β) was determined to be 1030 ± 10 °C by metallographic method in a commercial muffle furnace. The titanium alloy ingot was rolled at the temperature of 30–50 °C below T_β and then rapidly cooled in water (WQ). Afterwards, one hot-rolled specimen was rapidly heated to 900 °C while the other one was rapidly heated to 920 °C with a heating rate of about 15 °C/s, and then the two specimens were solution-treated for 1 h in Gleeble 3500 physical simulator with an argon atmosphere followed by rapid cooling in water. The two solution-treated specimens were labeled as 900 °C/1 h/WQ (1#) and 920 °C/1 h/WQ (2#). Finally, 1# and 2# solution-treated specimens were heated to 550 °C with a heating rate of 5 °C/min and aged for 6 h followed by air cooling (AC). The completely heat-treated specimens were labeled as 900 °C/1 h/WQ + 550 °C/6 h/AC (3#) and 920 °C/1 h/WQ + 550 °C/6 h/AC (4#). By specially designing the solution and aging treatment parameters, the hierarchical microstructure composed of α_p regions and β_t regions was prepared.

The specimens for quasi-static tensile tests were machined from the solution-treated and completely heat-treated titanium alloys by wire cutting process. The schematic diagram of the specimens is shown in Fig. 1. The yield strength, ultimate tensile strength, and fracture elongation of the titanium alloys under different conditions were measured at room temperature and a strain rate of 10^{-3}/s using an Instron Universal Testing machine (Instron 5500R, Instron, Boston, USA) with the loading direction parallel to the rolling direction (RD), and an extensometer was loaded to record deformation.

Microstructural characterization was performed via optical microscopy (OM) and field emission gun scanning electron microscopy (FEGSEM; Quanta 200FEG, FEI, Hillsboro, USA), and the observation direction was parallel to the normal direction (ND). The specimens for the OM (ZEISS Axiovert 25, Carl Zeiss AG, Jena, Germany) and SEM observations were mechanically polished after being ground with various (400–2000) grits of SiC paper, and then they were etched in Kroll's reagent (10 mL HF, 30 mL HNO_3, and 200 mL H_2O). In addition, all the SEM

Table 1
The composition of the titanium alloy utilized in the present study(wt. %).

Element	Al	Cr	Mo	Fe	Zr	Sn	Zn	O	N	H	C	Ti
wt. %	5.12	2.5	4.48	0.52	1.8	1.1	2.9	0.08	0.02	0.002	0.01	Bal.

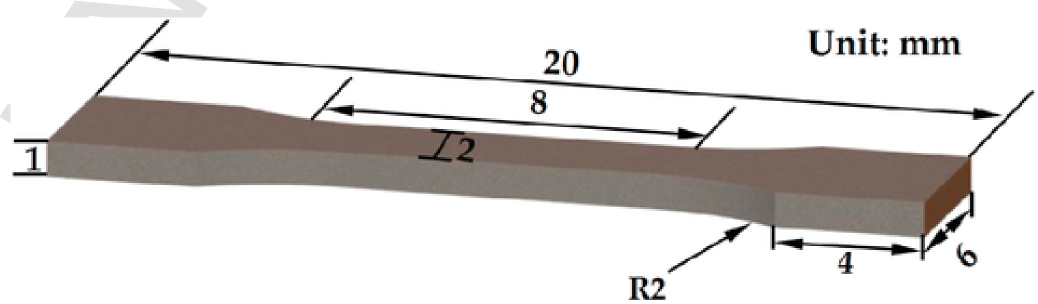

Fig. 1. The schematic diagram of the quasi-static tensile specimens.

images were obtained with SE detectors. Fine details of the microstructure were characterized by means of transmission electron microscopy (TEM) performed on a FEI Tecnai G2 microscope (FEI, Hillsboro, USA) operated at 200 kV. For TEM observation, the specimens were machined to a diameter of 3.0 mm using an electron discharge method and then polished to 100 μm thickness using various (400–2000) grits of SiC paper. Afterwards, the specimens were prepared via a twin-jet electrochemical polishing method with the chemical reagents of 6 mL $HClO_4$, 34 mL $CH_3(CH_2)_3OH$, and 60 mL CH_3OH. The metallographic analysis software Image Pro Plus V6.0 (Media Cybernetics, Washington, DC, USA) was used to analyze the microstructure of the materials quantitatively.

3. Results and discussion

3.1. Microstructure characteristics

Fig. 2 shows the microstructure of the hot-rolled Ti-4.5Mo-5.1Al-1.8Zr-1.1Sn −2.5Cr-2.9Zn alloy. It can be seen from Fig. 2(a) that the microstructure contains equiaxed α_p (identified by the dotted line) and β_t regions, and the average grain size of α_p is about 1.8 μm. Fig. 2(b) indicates that the microstructure of β_t regions is composed of β phase and acicular α_s embedded in β matrix. Acicular α_s was formed in the cooling process after hot-rolling. Fig. 2(c) shows the high magnification view of α_p regions, and some white precipitates are observed in α_p regions as indicated by the yellow arrow. In order to further identify the white precipitates, the bright-field TEM image near α_p regions was obtained and shown in Fig. 2(d). The selected area electron diffraction (SAED) pattern of the region in the red circle of Fig. 2 (d) is shown in Fig. 2 (e). It can be confirmed that the white precipitates are β phase. The phenomenon that β grains distribute in α_p regions may be attributed to some relatively enriched regions of β stable elements in α_p regions. During hot-rolling at high temperature, the β stable elements near these regions diffuse and aggregate to promote the nucleation of β phase. Finally, the nucleated β grains are retained in α_p regions during rapid cooling in water after hot-rolling.

The microstructures of the 900 °C/1 h/WQ (1#) and 920 °C/1 h/WQ (2#) solution-treated titanium alloys are shown in Fig. 3. Fig. 3(a)

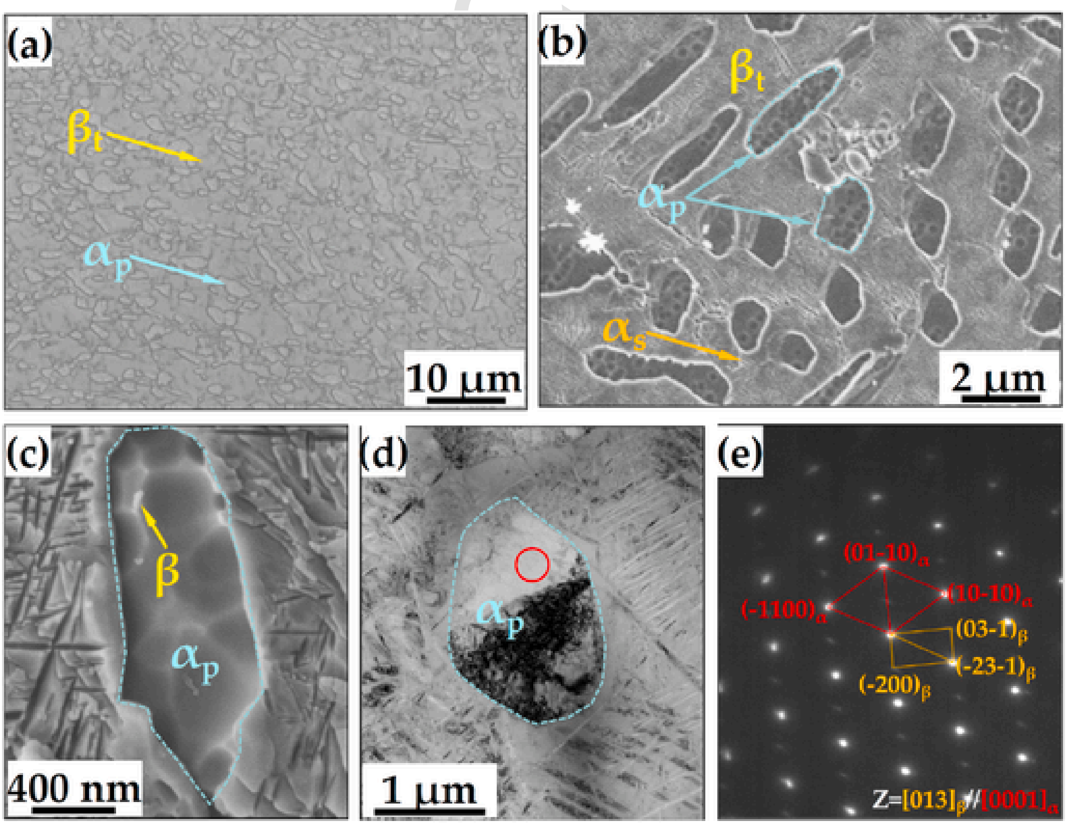

Fig. 2. The microstructure of the hot-rolled titanium alloy. (a) The OM image, (b) the SEM image, (c) the SEM image showing the high magnification view of α_p regions, (d) the bright-field TEM image of α_p regions and (e) the SAED of the red circle in (d). (For interpretation of the references to colour in this figure legend, the reader is referred to the Web version of this article.)

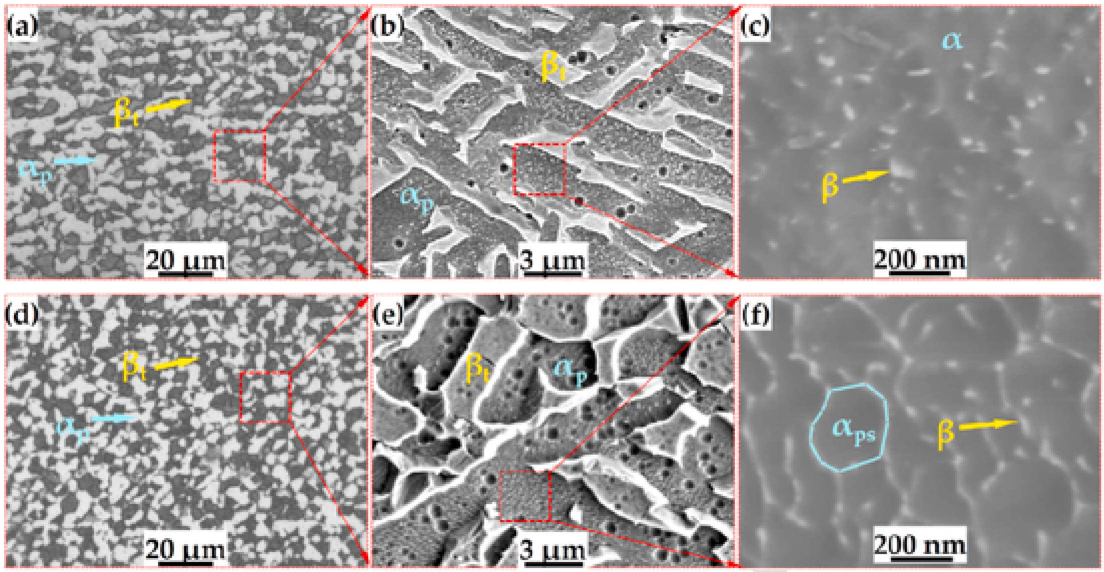

Fig. 3. The microstructures of solution treated titanium alloys. (a) and (d) the OM images of 1# and 2# titanium alloys, (b) and (e) showing the SEM microstructures in the red boxes in (a) and (c), and (c) and (f) showing the SEM microstructures of α_p regions in (b) and (e), respectively. (For interpretation of the references to colour in this figure legend, the reader is referred to the Web version of this article.)

shows the microstructure of 1# titanium alloy, which is composed of equiaxed α_p and β phase, and the average grain size of α_p is about 4.5 μm. Fig. 3(b) shows the high magnification view of the microstructure in the red box of Fig. 3(a). It can be seen that there is no finer structure in β_t regions, and β_t regions are composed of single β phase. However, a finer structure is observed in α_p regions, and the corresponding enlarged view is shown in Fig. 3(c). It can be seen that a large number of nano-scale β grains are dispersed in α_p regions. Fig. 3(d) shows the microstructure of 2# titanium alloy, and the average grain size of α_p is smaller (about 3.4 μm) compared with 1# titanium alloy. Fig. 3(e) indicates that similar to 1# titanium alloy, the β_t regions in 2# titanium alloy are also composed of single β phase. The enlarged view of the microstructure in the red box of Fig. 3(e) is shown in Fig. 3(f). In contrast to 1# titanium alloy, the β grains precipitated in α_p regions are connected with each other to separate α phase into finer α_{ps}, resulting in the hierarchical microstructure, which is composed of nano-scale equiaxed α_{ps} and β phase embedded between α_{ps}.

The microstructure of the 900 °C/1 h/WQ + 550 °C/6 h/AC (3#) completely heat-treated titanium alloy is shown in Fig. 4. Fig. 4(a) indicates that the average grain size of α_p in 3# titanium alloy is slightly larger (about 4.7 μm) compared with 1# solution-treated titanium alloy. Fig. 4(b) shows the high magnification view of the microstructure in the red box of Fig. 4(a). A finer structure is clearly observed in the α_p regions of 3# titanium alloy, and the corresponding detailed microstructure is shown in Fig. 4(c). Similar to 1# titanium alloy, due to the fact that the dispersed β grains are not connected with each other to separate α phase, no equiaxed α_{ps} is observed in the α_p regions of 3# titanium alloy. Particularly, compared with the β_t regions composed of single β phase in 1# and 2# solution-treated titanium alloys, a finer structure is found in the β_t regions of 3# titanium alloy, and the corresponding high magnification views are shown in Fig. 4(d)–4(f). It can be seen from Fig. 4(d) that there are a great number of acicular α_s in β_t regions, and the average thickness of acicular α_s is 80 nm–100 nm. Simultaneously, smaller acicular α_{ss} with an average thickness of 18 nm is

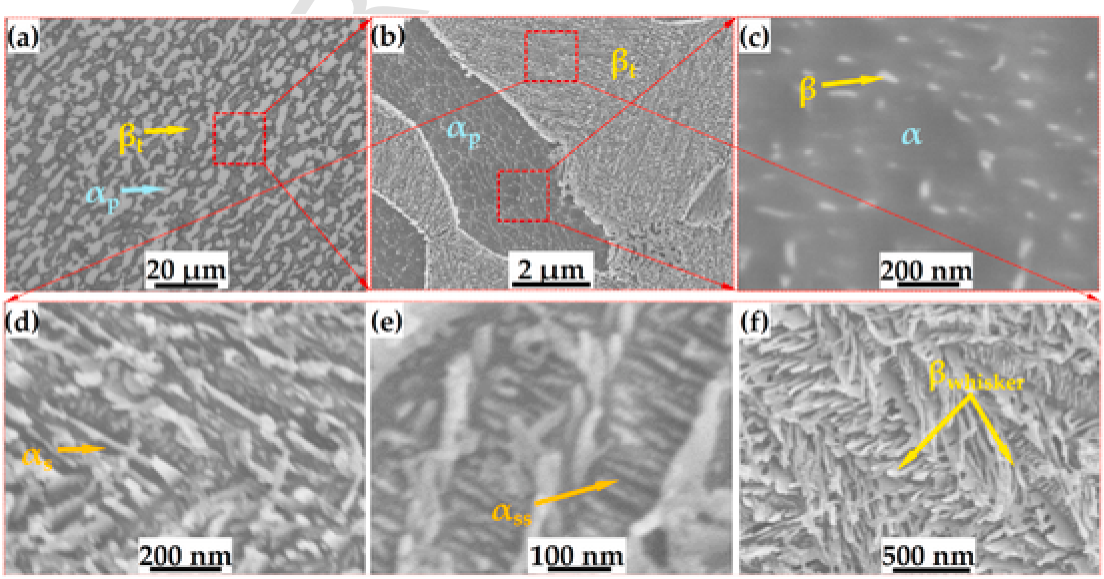

Fig. 4. The microstructure of 3# titanium alloy. (a) The OM image, (b) the SEM image, the SEM images showing the high magnification views of (c) α_p regions and (d)–(f) β_t regions.

found in the space of two α_s. Furthermore, after being repeatedly segmented by acicular α_s and α_{ss}, β phase exhibits obvious whisker characteristics, and the distribution characteristics of $\beta_{whisker}$ are closely related to acicular α phases.

The microstructure of the 920 °C/1 h/WQ + 550 °C/6 h/AC(4#) completely heat-treated titanium alloy is shown in Fig. 5. Compared with 2# solution-treated titanium alloy, the average grain size of α_p in 4# titanium alloy is smaller (about 4.1 μm), as shown in Fig. 5(a). Fig. 5(b) shows the high magnification view of the microstructure in the red box of Fig. 5(a). A finer structure is observed in the α_p regions of 4# titanium alloy, and the corresponding detailed microstructure is shown in Fig. 5(c). Similar to 2# titanium alloy, the equiaxed α_p in 4# titanium alloy are separated by β grains into a great number of finer equiaxed α_{ps} with an average grain size of 150 nm–200 nm. Particularly, in contrast to the β_t regions of solution-treated titanium alloys, a finer structure is found in the β_t regions of 4# titanium alloy, and the corresponding high magnification views are shown in Fig. 5(d)–5(f). Fig. 5(d) and (e) show the detailed microstructures of acicular α_s and α_{ss}, respectively. The average thickness of acicular α_s and α_{ss} is 50 nm–80 nm and 15 nm, respectively, which is smaller than that in 3# titanium alloy. In addition, as shown in Fig. 5(f), $\beta_{whisker}$ is also observed in the β_t regions of 4# titanium alloy, and the grain size of $\beta_{whisker}$ is determined by the distribution characteristics of α_s and α_{ss}. The above analysis clearly states that the hierarchical microstructure in β_t regions of the titanium alloys is formed during aging-treatment.

Table 2 more intuitively reflects the differences of the hierarchical microstructures in 1#, 2#, 3# and 4# titanium alloys. After solution-treatment at different temperatures, in addition to equiaxed α_p with different grain sizes in 1# and 2# titanium alloys, nano-scale equiaxed α_{ps} are also observed in the α_p regions of 2# titanium alloy. After aging-treatment, the average grain size of equiaxed α_p in 3# and 4# titanium alloys increases slightly, and the hierarchical microstructure is formed in β_t regions.

3.2. Formation mechanism of the hierarchical microstructures

A great number of β grains are dispersed in equiaxed α_p in the hot-rolled titanium alloy. The above hierarchical microstructures are prepared by specially designing the solution treatment parameter to control the diffusion rate of β stable elements in α_p regions and the aging treatment parameter to control the precipitation process of acicular α phases in β_t regions. The schematic diagram for the formation process of the hierarchical microstructures is shown in Fig. 6. The formation processes of the hierarchical microstructure formed in α_p regions during solution-treatment and that formed in β_t regions during aging-treatment will be discussed in detail, respectively.

The hierarchical microstructure in α_p regions is formed during solution-treatment. One hot-rolled specimen was rapidly heated to 900 °C while the other one was rapidly heated to 920 °C, and then the two specimens were solution-treated for 1 h followed by rapid cooling in water to prepare the hierarchical microstructure in α_p regions. This method has been applied in the study by Chen et al. [27] to obtain ultra-fine grain microstructures via the chemical boundary (CB) in steel. In their study, there was a nano-scale discontinuity in the Mn concentration at phase interfaces, and all the phase boundaries and many grain boundaries could be eliminated by rapid heating. Meanwhile, as a result of its sluggish diffusion, the spatial distribution of Mn was preserved, resulting in the formation of a high density of nonequilibrium CBs. In the following fast cooling process, these CBs divided the extensively coarsened austenite grains into a large number of ultra-fine domains, which distributed alternately in the enriched Mn regions or the depleted Mn regions, resulting in grain refinement in steel. In the present study, a lot of β grains discontinuously distributed in α_p regions of the hot-rolled titanium alloy, as shown in Fig. 6(a). It can be determined that there must be a discontinuity in the concentration of β stable elements. Therefore, α/α grain boundaries and α/β phase boundaries can be eliminated, and the CBs will be formed during rapid heating. In the subsequent process of rapid cooling in water, a large number of ultra-fine β grains will precipitate in α_p regions, as shown in Fig. 6(b) and (c).

In addition, in order to prepare different hierarchical microstructures in α_p regions, the solution temperature is set at 900 °C and 920 °C, respectively. At a higher solution temperature of 920 °C, β stable elements relatively fully diffuse and continuously concentrate to form a hierarchical microstructure, which is composed of equiaxed α_{ps} and β phase embedded between α_{ps}, as shown in Fig. 6(c). At a lower solution temperature of 900 °C, β grains dispersed in α_p regions are not connected with each other to separate α phase, thus no equiaxed α_{ps} is observed, as shown in Fig. 6(b). Simultaneously, increasing the solution temperature from 900 °C to 920 °C results in severe α→β phase transformation, which promotes β phase to grow. Consequently, 2# titanium alloy acquires a higher β phase fraction compared with 1# titanium alloy. Furthermore, severe α→β phase transformation leads to the sharp decrease of α_p grain size in 2# titanium alloy.

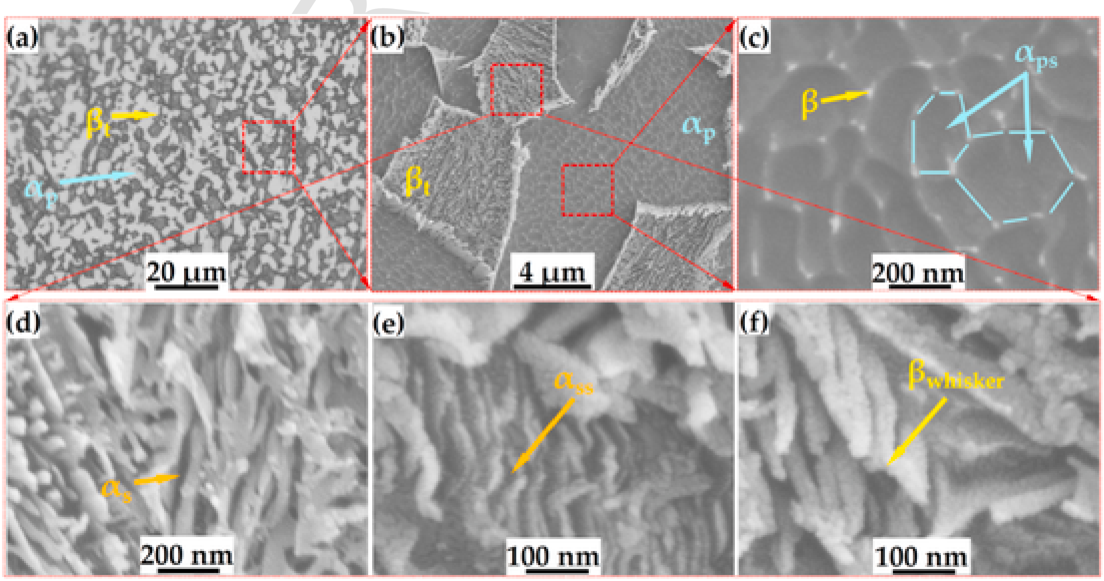

Fig. 5. The microstructure of 4# titanium alloy. (a) The OM image, (b) the SEM image, the SEM images showing the high magnification views of (c) α_p regions and (d)–(f) β_t regions.

Table 2
Microstructure characteristics of the titanium alloys under different conditions.

Alloy ID	Grain size in α_p region		Grain thickness in β_t region	
	α_p/μm	α_{ps}/nm	α_s/nm	α_{ss}/nm
1#	4.5 ± 0.15	–	–	–
2#	3.4 ± 0.20	150–200	–	–
3#	4.7 ± 0.08	–	80–100	18 ± 0.6
4#	4.1 ± 0.13	150–200	50–80	15 ± 0.9

(2) Hierarchical microstructure in β_t regions formed during aging-treatment

The hierarchical microstructure in β_t regions is formed during aging-treatment. Previous studies [7,28,29] have proved that acicular α_s precipitates during aging-treatment. The above 1# and 2# solution-treated titanium alloys are aging-treated at 550 °C for 6h followed by air cooling. In this case, α and β phases in titanium alloys reach an equilibrium state [30], that is, the contents of α phase in the completely heat-treated titanium alloys are consistent as well as β phase. In aging-treatment process, the hierarchical microstructure in α_p regions is almost unchanged due to the low aging temperature of 550 °C, as shown in Fig. 6(c). In fact, the microstructure characteristics of solution-treated titanium alloys have a significant influence on the formation process of the hierarchical microstructure in β_t regions, and the precipitation process of acicular α_s and α_{ss} is closely related to β phase fraction [31]. Larger β phase fraction supports more nucleation points for α_s during aging-treatment. With the growth of acicular α_s, once two α_s interconnect, the growth process is stopped immediately [32]. Therefore, finer and denser acicular α_s is observed in 4# titanium alloy because of a higher β phase fraction in 2# solution-treated titanium alloy. In particular, the β phase between two acicular α_s still provides nucleation points for smaller acicular α_{ss} after the growth process of acicular α_s stopped. Similar to acicular α_s, the growth process of acicular α_{ss} will be stopped by the obstruction of α_s, finally resulting in an α_{ss} structure with raft characteristics, as shown in Fig. 6(e) and (g). Meanwhile, after being repeatedly segmented by acicular α_s and α_{ss}, β phase in β_t regions exhibits special whisker characteristics.

3.3. Influence of hierarchical microstructure on mechanical properties

The quasi-static tensile tests were carried out on 1#, 2#, 3# and 4# titanium alloys, respectively. The test results are shown in Fig. 7. Fig. 7(a) shows the true stress-strain curves of the titanium alloys under different conditions. It can be seen that 1# titanium alloy acquires the lowest YS of 885 MPa and UTS of 1056 MPa, and the elongation is about 10.6%. Compared with 1# titanium alloy, the YS and UTS of 2# titanium alloy increase to 969 MPa and 1142 MPa, respectively, and the elongation is larger (about 12.8%). 3# titanium alloy exhibits moderate strength and the lowest elongation of only 4.1%. 4# titanium alloy acquires the highest YS of 1255 MPa and UTS of 1420 MPa. Compared with other titanium alloys, the elongation of 4# titanium alloy remains at an acceptable level (about 6%). The bar chart of the mechanical properties is shown in Fig. 7(b). It can be summarized that after aging-treatment, the strength of titanium alloy increases greatly, while the elongation decreases sharply. Compared with 3# titanium alloy, 4#

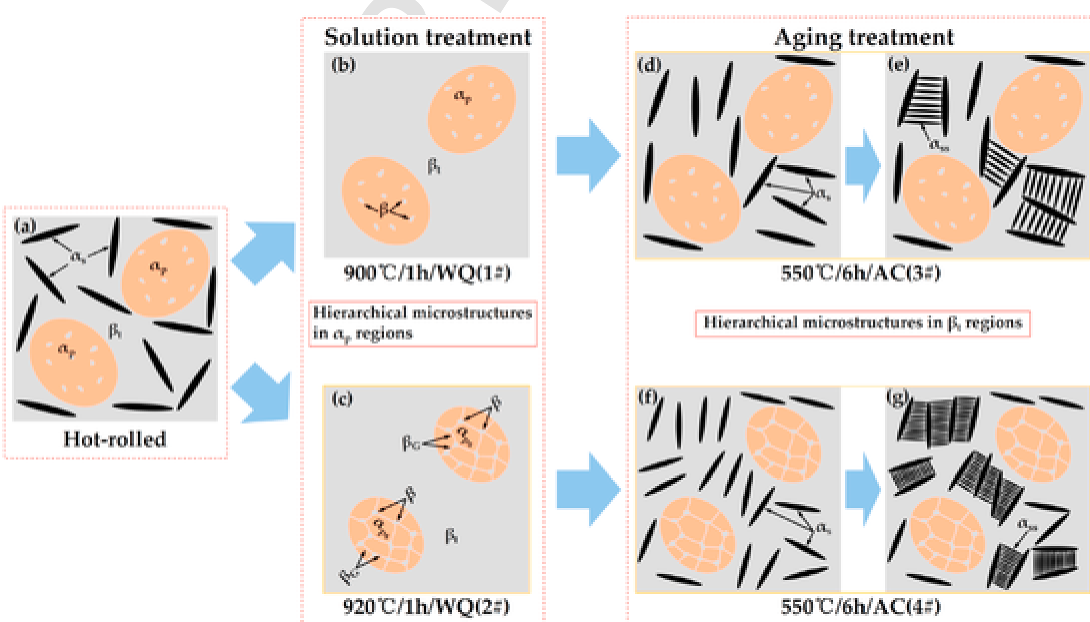

Fig. 6. The schematic diagram for the formation process of the hierarchical microstructures. The microstructures of the (a) hot-rolled, (b) 1# solution treated, (c) 2# solution treated, (d) and (e) 3# completely heat-treated, and (f) and (g) 4# completely heat-treated titanium alloys, respectively.

(1). Hierarchical microstructure in α_p regions formed during solution-treatment

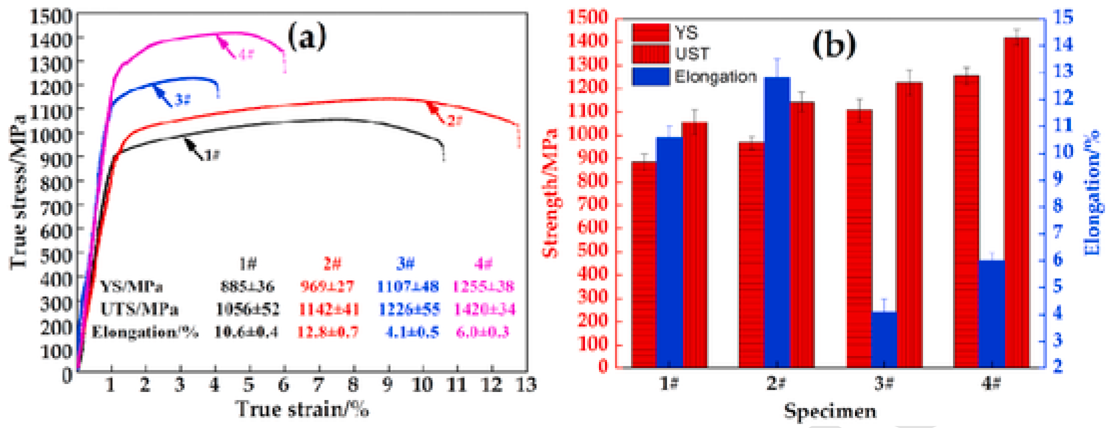

Fig. 7. The quasi-static mechanical properties of the titanium alloys under different conditions. (a) The true stress-strain curves and (b) the bar chart of the mechanical properties.

titanium alloy exhibits higher strength and plasticity, which overcomes the limitation of the strength-ductility trade-off to a certain extent.

The variation of the mechanical properties of the above titanium alloys under different conditions is closely related to the characteristics of the hierarchical microstructures. In α_p regions, the refinement of the equiaxed α_p and the formation of α_{ps} for β phase separating α phase can effectively enhance the strength and plasticity of titanium alloys. The refinement of equiaxed α_p significantly increases the grain boundary area and inhibits the propagation of cracks, thus improving the strength of titanium alloys. This is the grain boundary strengthening mechanism. In addition, the refinement of equiaxed α_p makes more equiaxed grains participate in the plastic deformation process, which is conducive to uniform plastic deformation, thus improving the plasticity of titanium alloys. Furthermore, compared with equiaxed α_p, nano-scale equiaxed α_{ps} will increase the grain boundary area more effectively. Therefore, based on the similar influence mechanism on mechanical properties, a large number of equiaxed α_{ps} can improve the strength and plasticity of titanium alloys more significantly.

In β_t regions, the refinement of acicular α phases will greatly improve the strength of titanium alloys but reduce the plasticity. During quasi-static tensile deformation, because β_t regions are separated into a larger number of extremely small cabinets by acicular α_s and α_{ss}, dislocation motion is restricted in these limited cabinets, and the maximum length of dislocation motion is the inter-particle spacing of two acicular α phases, that is, the grain size of the separated β phase [5,33–35]. In addition, the refinement and densifying of acicular α_s and α_{ss} will reduce the inter-particle spacing of two acicular α phases and further restrict the dislocation motion, thus significantly improving the strength of titanium alloys. This is the fine grain strengthening mechanism. However, the serious restriction of acicular α_s and α_{ss} on dislocation motion will promote the localized distribution of high density dislocations, leading to the uneven distribution of strain and the initiation of micro-cracks, which greatly reduces the plasticity of titanium alloys.

After solution-treatment, due to the fact that the average grain size of equiaxed α_p is smaller and a great number of nano-scale equiaxed α_{ps} precipitate in α_p regions, 2# titanium alloy exhibits higher strength and plasticity compared with 1# titanium alloy. After aging-treatment, the average grain size of equiaxed α_p in 3# titanium alloy is almost the same to that in 1# titanium alloy. This indicates that the extremely limited variation of grain size of equiaxed α_p will weakly change the strength and plasticity of titanium alloys, and the effect can be ignored. Furthermore, a great number of acicular α_s and α_{ss} in the β_t regions of 3# titanium alloy can significantly improve the strength but sacrifice the plasticity at the same time. For 4# titanium alloy, denser and finer acicular phases (α_s and α_{ss}) in β_t regions make 4# titanium alloy acquire higher strength compared with 3# titanium alloy. In addition, the refinement of equiaxed α_p and the formation of a large number of nano-scale equiaxed α_{ps} in the α_p regions of 4# titanium alloy can not only improve the strength, but also offset the negative effect of acicular phases on plasticity, thus resulting in an acceptable plasticity. Therefore, 4# titanium alloy exhibits higher strength and plasticity compared with 3# titanium alloy, which overcomes the limitation of the strength-ductility trade-off to a certain extent.

4. Conclusions

In this paper, a hierarchical microstructure, which was significantly different from the traditional microstructure of titanium alloys, was prepared by specially designing the solution and aging treatment parameters of a near β-type hot-rolled Ti-4.5Mo-5.1Al-1.8Zr-1.1Sn-2.5Cr-2.9Zn alloy, and it made the titanium alloy acquire super-high strength and acceptable plasticity. The major conclusions of the present study are summarized as follows:

(1) By controlling the diffusion rate of β stable elements in α_p regions during solution-treatment and the precipitation process of acicular phases in β_t regions during subsequent aging-treatment, a hierarchical microstructure was prepared, which was composed of α_p regions (nano-scale equiaxed α_{ps} + β phase embedded between α_{ps}) and β_t regions (acicular α_s with a thickness of dozens of nanometers + acicular α_{ss} with a thickness of 10 nm, distributed in the space of two α_s + $\beta_{whisker}$).
(2) Comparing to the solution treatment of 900 °C/1 h/WQ followed by the same aging-treatment, smaller α_p, a large number of nano-scale equiaxed α_{ps}, and denser and finer acicular α phases were found in the 920 °C/1 h/WQ + 550 °C/6 h/WQ titanium alloy.
(3) The combined strengthening effect of equiaxed α_p refinement, nano-scale equiaxed α_{ps} and acicular α phases made the hierarchical microstructure exhibit super-high YS of 1255 MPa and UTS of 1420 MPa. Meanwhile, the refined equiaxed α_p and nano-scale equiaxed α_{ps} could offset the negative effect of acicular α phases on plasticity, hence to maintain the plasticity at an acceptable level (elongation: 6%).

Data availability

The raw/processed data required to reproduce these findings cannot be shared at this time due to legal or ethical reasons.

CRediT authorship contribution statement

Xinjie Zhu: Data curation, Writing – original draft, Visualization. **Qunbo Fan:** Writing – review & editing, Resources, Supervision. **Haichao Gong:** Investigation, Validation. **Jiayao Ying:**

Investigation. **Hong Yu:** Validation. **Xingwang Cheng:** Software. **Lin Yang:** Investigation, Validation. **Liu Yang:** Investigation. **Nan Li:** Supervision. **Jishan Li:** Supervision.

Declaration of competing interest

The authors declare that they have no known competing financial interests or personal relationships that could have appeared to influence the work reported in this paper.

Acknowledgments

This work was financially supported by the Chongqing Nature Science Foundation(Grant No. Cstc2020jcyj-msxmX0094), and the Joint Research Programs between Beiarusian Republican Foundation for Fundamental Research and Beijing Institute of Technology “BRFFR-BIT-2020” (Grant No. BITBLR2020004).

References

[1] I.G. Crouch, The Science of Armour Materials, 2017, pp. 117–166, Elsevier: Woodhead Publishing.
[2] R.R. Boyer, Attributes, characteristics and application of titanium and its alloys, J. Occup. Med. 62 (2010) 21–24.
[3] A. Devaraj, V.V. Joshi, A. Srivastava, et al., A low-cost hierarchical nanostructured beta-titanium alloy with high strength, Nat. Commun. 7 (2016) 11176.
[4] W.G. Zhu, J. Lei, Z.X. Zhang, et al., Microstructural dependence of strength and ductility in a novel high strength β titanium alloy with Bi-modal structure, Mater. Sci. Eng. 762 (2019) 138086.
[5] Z. Zhao, J. Chen, H. Tan, et al., Achieving superior ductility for laser solid formed extra low interstitial Ti-6Al-4V titanium alloy through equiaxial alpha microstructure, Scripta Mater. 146 (2018) 187–191.
[6] G. Srinivasu, Y. Natraj, A. Bhattacharjee, et al., Tensile and fracture toughness of high strength β Titanium alloy, Ti-10V-2Fe-3Al, as a function of rolling and solution treatment temperatures, Mater. Des. 47 (2013) 323–330.
[7] S.A. Mantr, D. Choudhuri, T. Alam, et al., Tuning the scale of α precipitates in β-titanium alloys for achieving high strength, Scripta Mater. 154 (2018) 139–144.
[8] I.V. Okulov, H. Wendrock, A.S. Volegov, et al., High strength beta titanium alloys: new design approach, Mater. Sci. Eng. 628 (2015) 297–302.
[9] A.F. Alhosseini, M.K. Keshavarz, Y. Mazaheri, et al., Strengthening mechanisms of nano-grained commercial pure titanium processed by accumulative roll bonding, Mater. Sci. Eng. 693 (2017) 164–169.
[10] M. Markushev, D. Nugmanova, O. Sitdikov, et al., Structure, texture and strength of Mg-5.8Zn-0.65Zr alloy after hot-to-warm multi-step isothermal forging and isothermal rolling to large strains, Mater. Sci. Eng. 709 (2018) 330–338.
[11] Y. Fu, W.L. Xiao, J.S. Wang, et al., A novel strategy for developing α+ β dual-phase titanium alloys with low Young’s modulus and high yield strength, J. Mater. Sci. Technol. 76 (2021) 122–1278.
[12] D.K. Chouhan, S. Biswas, A.K. Singh, et al., High tensile strength-ductility combination in cold multiaxial plane-strain forged and rolled nanostructured titanium, Materialia 11 (2020) 100698.
[13] W. Daniel, W. Krzysztof, C. Robert, et al., Microstructure-strength relationship of ultrafine-grained titanium manufactured by unconventional severe plastic deformation process, J. Alloys Compd. 837 (2020) 155576.
[14] S. Zherebtsov, E. Kudryavtsev, S. Kostjuchenko, et al., Strength and ductility-related properties of ultrafine grained two-phase titanium alloy produced by warm multiaxial forging, Mater. Sci. Eng. 536 (2012) 190–196.
[15] I.V. Ratochka, I.P. Mishin, O.N. Lykova, et al., Effect of annealing on the superplastic properties of ultrafine-grained Ti-5Al-5V-5Mo-1Cr-1Fe alloy, Mater. Sci. Eng. 803 (2021) 1940511.
[16] V.N. Chuvil’deev, V.I. Kopylov, A.V. Nokhrin, et al., Study of mechanical properties and corrosive resistance of ultrafine-grained α-titanium alloy Ti-5Al-2V, J. Alloys Compd. 723 (2017) 354–367.
[17] A.J. Huang, G.P. Li, Y.L. Hao, et al., Acicular α2 precipitation induced by capillarity at α/β phase boundaries in Ti-14Al-2Zr-3Sn-3Mo-0.5Si titanium alloy, Acta Mater. 51 (2003) 4939–4952.
[18] H. Fujii, Strengthening of α + β titanium alloys by thermomechanical processing, Mater. Sci. Eng. 243 (1998) 103–108.
[19] O.M. Ivasishin, P.E. Markovsky, Y.V. Matviychuk, et al., A comparative study of the mechanical properties of high-strength β-titanium alloys, J. Alloys Compd. 457 (2008) 296–309.
[20] Z.Y. Wang, L.B. Liu, D. Wu, et al., α″ phase-assisted nucleation to obtain ultrafine α precipitates for designing high-strength near-β titanium alloys, Trans. Nonferrous Metals Soc. China 30 (2020) 2681–2696.
[21] C. Cheng, K. Kadoi, H. Fujii, et al., Improved strength and ductility balance of medium-carbon steel with chromium and titanium fabricated by friction stir welding process, Mater. Sci. Eng. 803 (2021) 140689.
[22] X. Luo, L.H. Liu, C. Yang, et al., Overcoming the strength-ductility trade-off by tailoring grain-boundary metastable Si-containing phase in β-type titanium alloy, J. Mater. Sci. Technol. 68 (2021) 112–123.
[23] Y.D. Shi, M. Li, D.F. Guo, et al., A hierarchical and multiphase nanolaminated alloy with an excellent combination of tensile properties, Mater. Sci. Eng. 615 (2014) 464–468.
[24] Y. Yang, P. Castany, Y.L. Hao, et al., Plastic deformation via hierarchical nano-sized martensitic twinning in the metastable β Ti-24Nb-4Zr-8Sn alloy, Acta Mater. 194 (2020) 27–39.
[25] W. Xue, G. Yang, S. Bi, et al., Construction of caterpillar-like hierarchically structured Co/MnO/CNTs derived from MnO2/ZIF-8@ZIF-67 for electromagnetic wave absorption, Carbon 173 (2021) 521–527.
[26] L.M. Kang, Y.J. Cai, X.C. Luo, et al., Bimorphic microstructure in Ti-6Al-4V alloy manipulated by spark plasma sintering and in-situ press forging, Scripta Mater. 193 (2021) 43–48.
[27] R. Ding, Y.J. Yao, B.H. Sun, et al., **Chemical boundary engineering: a new route toward** lean, ultrastrong yet ductile steels, Science Advances 6 (2020) 1–8.
[28] L. Ren, W.L. Xiao, H. Chang, et al., Microstructural tailoring and mechanical properties of a multi-alloyed near β titanium alloy Ti-5321 with various heat treatment, Mater. Sci. Eng. 711 (2018) 553–561.
[29] S. Shekhar, R. Sarkar, S.K. Kar, et al., Effect of solution treatment and aging on microstructure and tensile properties of high strength β titanium alloy, Ti-5Al-5V-5Mo-3Cr, Mater. Des. 66 (2015) 596–610.
[30] X. Zhang, H.C. Kou, J.S. Li, et al., Evolution of the secondary a phase morphologies during isothermal heat treatment in Ti-7333 alloy, J. Alloys Compd. 577 (2013) 516–522.
[31] K. Wang, M.Q. Li, Effects of heat treatment and hot deformation on the secondary α phase evolution of TC8 titanium alloy, Mater. Sci. Eng. 613 (2014) 209–216.
[32] C. Dichtla, Z.B. Zhang, H. Gardner, et al., Element segregation and α_2 formation in primary α of a near-α Ti-alloy, Mater. Char. 164 (2020) 110327.
[33] Y.M. Cui, C.H. Li, C.S. Zhang, et al., Effect of initial microstructure on the micromechanical behavior of Ti-55531 titanium alloy investigated by in-situ high-energy X-ray diffraction, Mater. Sci. Eng. 772 (2020) 138806.
[34] S. Acharya, S. Bahl, S. Singh Dabas, et al., Role of aging induced α precipitation on the mechanical and tribocorrosive performance of a β Ti-Nb-Ta-O orthopedic alloy, Mater. Sci. Eng. C 3 (2019) 109755.
[35] X.G. Fan, M. Meng, P.F. Gao, et al., Coupled effects of deformation and cooling on the evolution of primary and secondary alpha of two-phase Ti-alloys, Mater. Sci. Eng. 710 (2018) 271–279.